Thermochimica Acta 477 (2008) 48–53

Contents lists available at ScienceDirect

Thermochimica Acta

journal homepage: www.elsevier.com/locate/tca

Nano-calorimetry of small-sized biological samples

J. Lerchner[a,*], A. Wolf[a], H.-J. Schneider[a], F. Mertens[a], E. Kessler[b], V. Baier[b], A. Funfak[c], M. Nietzsch[d], M. Krügel[d]

[a] TU Bergakademie Freiberg, Inst. Physical Chemistry, Leipziger Str. 29, D-09596 Freiberg, Germany
[b] Inst. Photonic Technologies IPHT, Albert-Einstein-Str. 9, D-07742 Jena, Germany
[c] TU Ilmenau, Inst. Physics, PF 100565, D-98684 Ilmenau, Germany
[d] "Eurotronics" Gesellschaft f. wiss. Gerätebau mbH, Weissenfelser Str. 67, D-04229 Leipzig, Germany

ARTICLE INFO

Article history:
Received 28 April 2008
Received in revised form 11 August 2008
Accepted 14 August 2008
Available online 28 August 2008

Keywords:
Chip-calorimetry
Biofilm
Pseudomonas putida
Staphyloccocus aureus
Zebra fish embryos

ABSTRACT

A miniaturized calorimeter with a signal noise of less than 10 nW is presented for the first time. The outstanding signal performance was obtained due to an elaborated temperature control inside the system. With a sample volume of around 6 μl a specific heat flow detection limit of <2 mW l^{-1} was achieved, which is a prerequisite for promising microbiological applications. The performance of the new calorimeter is demonstrated by investigations of the metabolic heat production of biofilms, bacteria cultured in suspensions, and single fish embryos.

1. Introduction

Bio-calorimetry is important in the field of thermophysical methods because it provides direct information about the physiological state of organisms and is helpful for the recognition of metabolic pathways [1]. Furthermore, a label-free detection of enzyme activities is possible. With the invention of miniaturized calorimeters, which are usually built in silicon chip technology, some weaknesses of conventional calorimeters were overcome, such as high-cost, high sample volume, and low dynamics [2]. Even though there are no chip calorimeters on the market yet, the less material expenditure for their construction suggests smaller costs. The need of high sample volume is a weakness if highly elaborated samples as immobilisates, single cells or encapsulated microorganisms should be investigated. For example, using chip calorimeters it is now possible to study the metabolic activity of small individual small multi-cellular organisms, small samples of both microbial suspensions and attached cells. The better dynamics of chip calorimeters concern the time constant of the heat flow detector, the possibility of integration of fast micro-fluidics as well as the small inertia of the thermostat. The letter is a precondition for a highly dynamic temperature control. If the calorimeter is used as a heat flow sensor located away from the sample source (e.g. a bioreactor) and connected via a sample loop, the outstanding dynamic behaviour of chip calorimeters permits a sample transfer time in the scale of seconds. That avoids alteration of the sample in the flow line.

The signal-to-noise ratio decreases with progressive miniaturization [3]. Hence, the resolution of the heat flow measurement must be in the lower nano-Watt range if chip calorimeters are to be suitable for biological or biochemical applications. In general, a volume specific resolution of a few mW l^{-1} is required for relevant microbiological investigations.

In the past, some descriptions of chip calorimeters have already been published [4–8] for bio-applications. Among them is a device which exhibit an excellent signal resolution, but its sample volume is too small (13 nW but only 0.7 nl [4]) to provide a signal-to-noise ratio which is acceptable for general biological measurements. In the present paper, a new version of a silicon chip-based calorimeter is described with a heat flow detection limit of about 10 nW. To our knowledge, this is the best value published to date. It is noteworthy that this signal resolution was achieved for sample volumes of some μl, which provides a volume specific value of less than 2 mW l^{-1}. On the other hand, this sample volume is still small enough to ensure a sufficiently low time constant of the calorimeter.

As recently outlined [3], the signal resolution in moderately miniaturized calorimeters is still considerably dependent

* Corresponding author. Tel.: +49 3731 39 2125; fax: +49 3731 39 3588.
E-mail address: Johannes.Lerchner@chemie.tu-freiberg.de (J. Lerchner).

0040-6031/$ – see front matter © 2008 Elsevier B.V. All rights reserved.
doi:10.1016/j.tca.2008.08.007

on the precision of the temperature management. Therefore, the emphasis on the current calorimeter development was placed on the improvement of the thermostat system. The sophisticated design of the new thermostat system provides a temperature stability near the reference junctions of the thermopiles of better than 40 μK during a time period of more than 40 min, which is the essential for the achieved heat flow detection limit. Additional new features of the calorimeter are a removable measurement chamber and a fluidic system appropriate for flow-injection procedures. Removable chambers allow a very comfortable handling of immobilized samples as for example biofilms, encapsulated microorganisms, enzymes, and individual small multi-cellular species. The relevance of the achieved performance of the calorimeter will be demonstrated by investigations of the metabolic activity of biofilms, bacterial growth at low cell density as well as by a study of the metabolism of zebra fish embryos.

2. Experimental

2.1. The calorimetric device

The device is a significant improvement of a recently described flow-through chip calorimeter [9] which comprises a silicon chip-based heat flow transducer mounted inside a thermostat, a measurement chamber attached at the chip, two fluid control units, and different signal processing components. Due to its outstanding performance the silicon chip transducer used in the calorimeter is the same one as in the previously presented developments [10]. It consists of four distinct independently readable thermopile sections (TP1–TP4) with an electronically determinated noise equivalent power of 8 nW (band width 1 Hz). The heat flow transducer chip is glued onto a copper plate and equipped with a printed circuit board is located inside two nested thermostats. The newly designed thermostat is schematically depicted in Fig. 1. In order to suppress disturbances due to fluid injection pulses as well as to minimize temperature gradients inside the thermostat both the fluid heat exchanger and the chip module are located close together at a small sized temperature controlled platform which is part of the copper made body of the thermostat. The applied PID control algorithm was optimized based on a system identification procedure (MATLAB, MathWorks Inc., Natick, MA, USA). The temperature of the thermostat can be fixed at 25 and 37 °C, respectively. The control temperature sensor and cylindrical heating elements are inserted into the platform. An additional temperature sensor is placed inside the carrier plate of the chip module (chip reference temperature). A precise temperature equilibration of the fluid flow is performed using micro-mechanically manufactured heat exchangers (IPHT e.V., Jena, Germany) fixed at the lower side of the platform.

Fig. 2 shows some features of the new micro-machined flow-through measurement chambers. They consist of polymethylmethacrylate (PMMA, Goodfellow GmbH, Bad Nauheim, Germany) and are provided with a flow channel inside. The chambers have two fluid inlets and can be mounted removable onto the top of the thermopile chip. The flexible arrangement of the measurement chamber permits new important applications of the device: Non-fluid samples (immobilisates, encapsulated bacteria, individual small multi-cellular organisms) can easily be introduced via the frontal port. For the measurement of associated reactants (catalysts, bacteria) it is possible to keep defined internal surface conditions by renewing of the top and the bottom cover foils after each experiment. Furthermore, the thin-film membrane of the thermopile chip is protected against mechanical stress induced by pressure pulses during fluid injection. The volume of the flow channel ranges

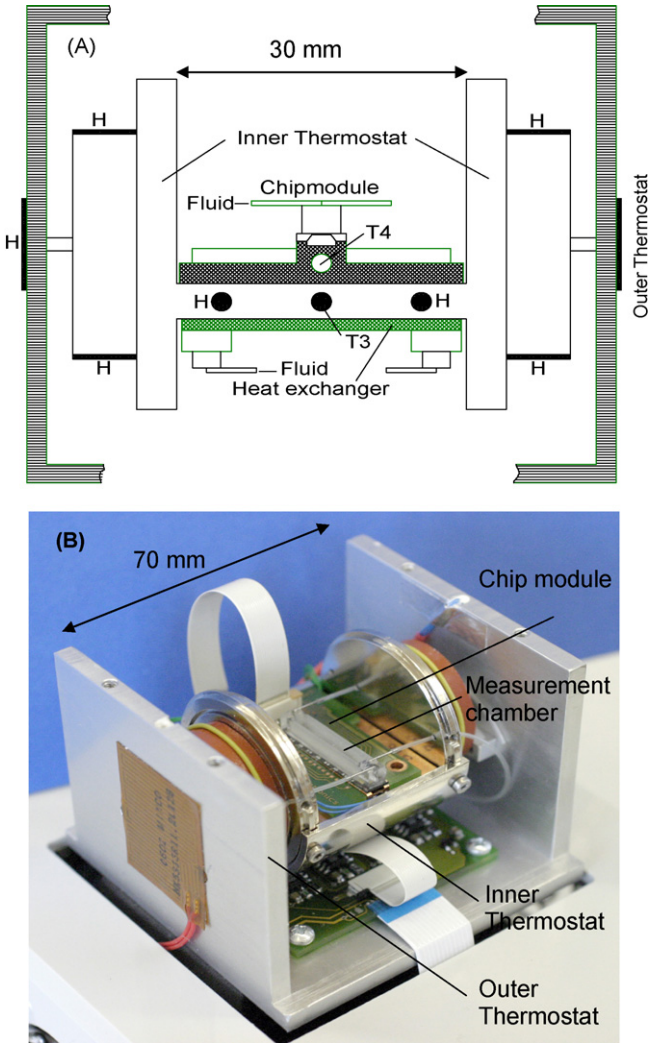

Fig. 1. Thermostat system (A: schema, B: photograph, without lids, H: heater, T3 and T4: thermistors, the thermistors T1 and T2 which are not shown here are located in the outer thermostat).

from 10 to 26 μl dependent on the chosen channel height. The bottom of the channel is usually covered by a PMMA foil (Goodfellow) of 50 μm thickness but also other materials can be used if required by the application (e.g. electrical conductive polymers for special biofilm studies). A sufficiently good thermal contact between chamber and chip membrane is achieved by a paraffin film attached at the bottom chamber foil. If the calorimeter is used for measurements of extremely small heat flows the channel is almost completely filled with a PMMA filler piece in the TP4 section (Fig. 2). Only a small gap of 0.1 mm between the filler piece and the top of the channel is still available to ensure the fluid flow. Due to the filler thermopile TP4 is only minimal affected by the heat flow of the studied process. On the other hand, external temperature perturbations cause similar disturbances on the four thermopile signals. Therefore, the temperature caused disturbances in the signals from TP1 to TP3 can be eliminated by subtracting the TP4 signal.

The average calorimetric sensitivity of the device, which depends on the height of the flow channel [3], was determined using the base-catalyzed hydrolysis of methylparaben [11]. Joule heating calibrations were performed in order to verify vertical sensitivity gradients inside the channel, which was important for the quantification of heat production of biofilms cultivated inside the

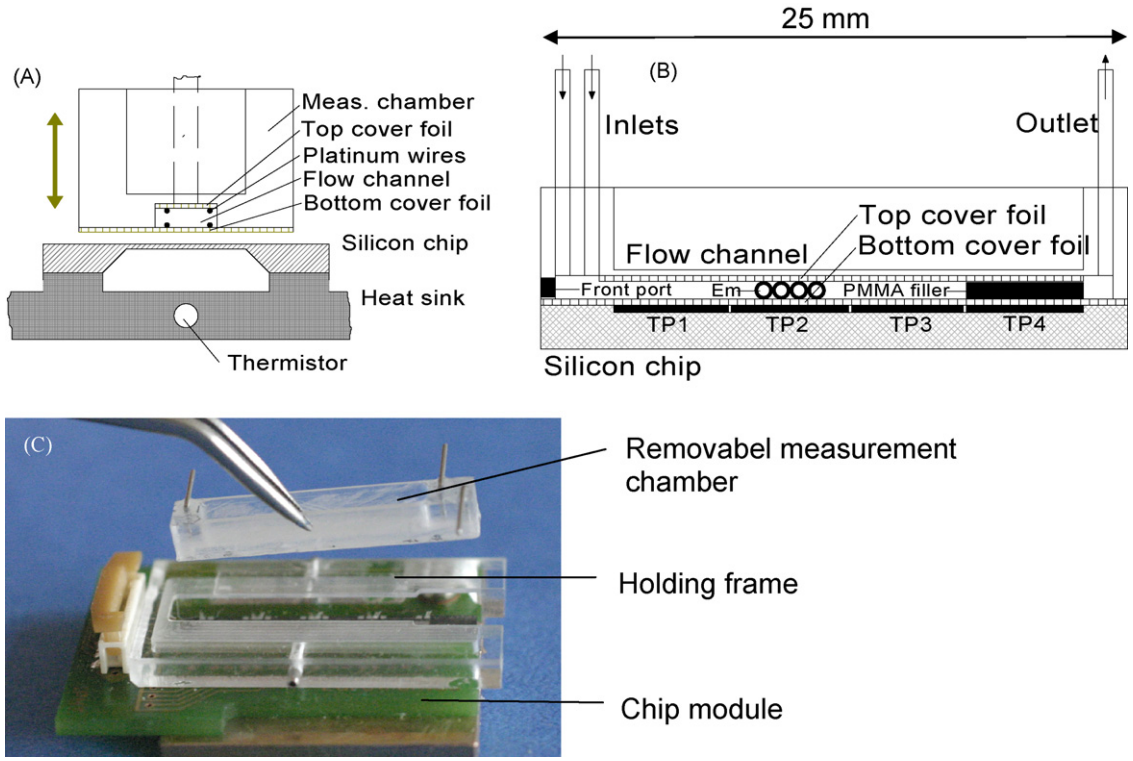

Fig. 2. Features of the measurement chambers. (A) Cross-section of the chamber and the silicon chip (separated). The platinum wires are optional for Joule heating calibration. (B) Longitudinal-section of the attached chamber and silicon chip with the four thermopile sections TP1–TP4, an optional frontal port for the introduction of immobilisates and an optional inert filler (PMMA) in the TP4 section. Em: position of the fish embryos. (C) Photograph of the chip module with removed measurement chamber.

channel. For this several measurement chambers were equipped with platinum wires attached at both the top and the bottom of the channel.

Every fluid control unit comprises a membrane pump (50 μl stroke), a piston pump (280 μl stroke), and three inert valves (all components from LEE Company, Westbrook, CT, USA). In case of a flow-injection regime the sample fluid (e.g. bacterial suspension or pharmaceuticals) is absorbed by the membrane pump and fast injected into a sample loop of 60 μl. After the sample loop is sufficiently flushed with the sample fluid the contents of the sample loop is continuously forced into the detection unit by the piston pump which was filled before with an appropriate carrier liquid (e.g. nutrient solution). The dead volume of the fluidic components inside the calorimetric unit is 30 μl. A time delay of less than 1 min between start of sampling and signal generation can be achieved with a typical volume flow rate of 100 μl min^{-1}. The reduction of the sample transfer time delay is important in the case of biological samples because of possible oxygen or substrate depletion during the transfer into the calorimeter.

2.2. Measurement protocols

As a demonstration of the calorimeter performance we have measured the metabolic heat production rate of several biological species including suspended and attached bacteria as well as fish embryos. The presented results were obtained in the framework of different research projects. Details of the projects are given elsewhere [12,13].

Pseudomonas putida PAW340 was used for the calorimetric study of biofilm activities [12]. For the cultivation of the biofilm several measurement chambers were connected in series with a laboratory bioreactor. In a bioreactor, *P. putida* was grown on sodium benzoate as carbon source and the bacteria suspension was continuously pumped through the chambers (for details see [12]). For the measurement of the activity of the biofilm, selected chambers were disconnected and mounted inside the calorimeter. Heat flow signals were initiated by the injection of nutrient solution through the measurement chamber. A stopped-flow measurement regime with consecutively alternating injection and waiting periods was carried out.

To analyze the lower limit of the detection of the metabolic heat production of suspended bacteria the growth of the strain *Staphylococcus aureus* was measured at low cell concentration. The bacteria were inoculated in complex media. The starting cell concentration was approximately 10^5 cells/ml. Several aliquots of the bacterial sample were incubated at 37 °C. Every hour a 1 ml aliquot was taken for a calorimetric measurement. Simultaneously the cell count (cfu number, colony forming units) was determined by conventional plating technique.

Adult zebra fish (*Danio rerio*) were obtained from Biotechnology Center and Cluster of Excellence/DFG Research Center for Regenerative Therapies Dresden, CRTD Dresden University of Technology (Michael Brand).

Table 1
Experimentally determined and calculated sensitivities for chambers with different bottom cover foils (1.2 mm channel height)

Material	S_{exp} (V W^{-1})	S_{calc} (V W^{-1})
Steel (40 μm)	2.0	1.4
Steel (7 μm)	3.0	3.1
Gold (20 μm)	0.4	0.3
Mylar (6 μm)	5.5	5.4
PMMA (50 μm)	5.4	5.3
Glued chamber	5.5	

For comparison the sensitivity for a glued chamber is included.

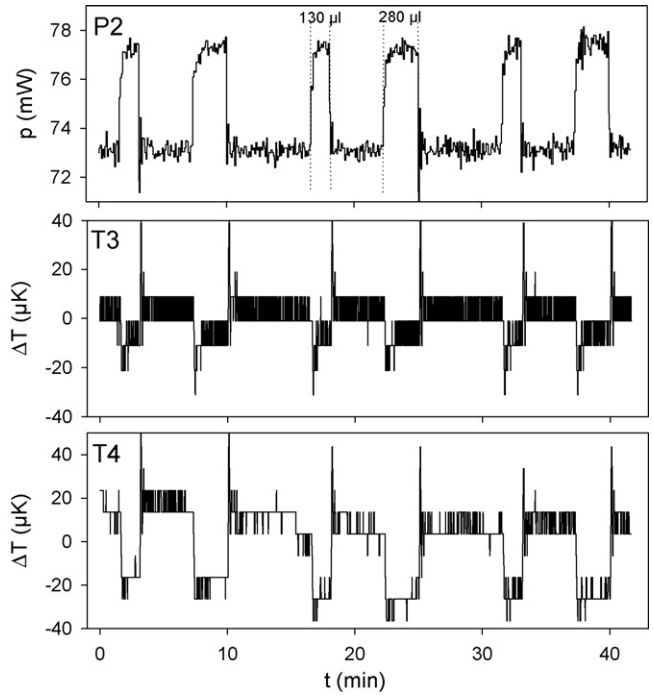

Fig. 3. Dynamic behaviour of the inner thermostat with respect to fluid flow pulses. P2: controller action due to the injection of 130 μl and 280 μl of nutrient solution at a flow rate of 50 μl min^{-1}. T3 and T4: progressions of the controller temperature and the chip reference temperature, respectively.

After fertilization of the eggs, the resultant embryos were transferred to E3 medium (34 mL buffer (5 mM NaCl, 0.17 mM KCl, 0.33 mM $CaCl_2{\cdot}2H_2O$, $MgSO_4{\cdot}7H_2O$) and 4 mL of 0.01% methylene blue solution per litre of distilled water) and incubated at 26 °C. Two and three days after fertilization embryos were randomly selected. Prior to the measurement the selected embryos were inserted into the chamber through the frontal port. Then the port was plugged by a stopper. The channels were especially prepared to fix the embryos in the thermopile TP2 section. Periodic injections of E3 medium were performed to stimulate the metabolism.

3. Results and discussion

3.1. Calorimetric sensitivity

Calorimetric sensitivities were determined [11] with different materials and thicknesses of the cover foil in order to optimize the chamber design. For comparison, relative sensitivities were calculated based on a heat exchange model of the calorimeter which was recently described [3]. As it can be derived from Table 1, chambers covered with thin polymer foils do not display a significantly lower sensitivity in comparison with chambers directly glued onto the chip. As expected, Joule heating calibrations using the attached platinum wires yielded lower sensitivities at the top of the channel than near the bottom. The difference of the sensitivity decreases from 20 to 3% for channel heights of 1.2–0.5 mm, respectively. Therefore, chambers with small channel height were used for the biofilm investigations to ensure sufficiently uniform sensitivities for all adhesion sites. Furthermore, model-based calculations have shown that the influence of the paraffin film attached for thermal contact between chamber and chip membrane has no significant effect on the sensitivity.

3.2. Signal performance

As mentioned above the measurement of the metabolic heat production in micro-sized samples requires an extremely high signal resolution in order to achieve a sufficiently high signal-to-noise ratio. The ultimate limit of the heat flow detection is mainly determined by the Johnson noise of the transducer and the noise of the amplifier. In sum, we found 35 nV (standard deviation) corresponding to a noise equivalent power of 7 nW (sensitivity 5 V W^{-1}). An elaborated temperature management is necessary to avoid dominating temperature perturbation effects. The temperature performance that we obtained with the described experimental arrangement is illustrated by Fig. 3, which shows the progression of the temperature at two positions during fluid injection. Temperature sensor T3 is the controller sensor and is located inside the carrier platform of the thermostat whereas T4 represents the temperature inside the chip module near the reference junctions of the thermopiles. The fast changes of the controller heat power P2, which are initiated by nearly rectangular liquid flow pulses in the heat exchanger, confirm the excellent dynamics of the optimized PID algorithm. The distortion of the controller temperature T3 is about 10 μK and the integrative part of the PID algorithm sufficiently suppresses steady deviations of the controller temperature during the fluid flow. The effect in T4 is stronger (40 μK) because the non-uniform dissipation of the controller heat power produces varying temperature gradients inside the carrier platform.

Usually a stopped-flow measurement regime with consecutively, alternating injection and waiting periods was applied in order to correct base line drifts. Two typical shapes of the signals are displayed in Fig. 4. Injections were performed with a rate of 50 μl min^{-1}. The signal in Fig. 4A stands for the measure-

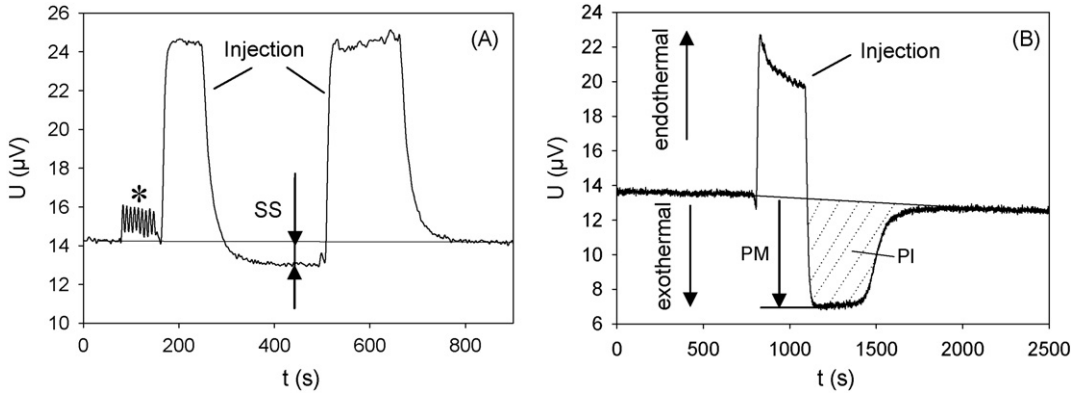

Fig. 4. Typical shapes of calorimetrical signals obtained from living organisms. (A) Steady-state heat power production of a diluted bacterial suspension (SS: signal shift after injection of bacteria, *: effect of pump actions). (B) Transient heat power production after injection of nutrient (PM: peak maximum, PI: exothermal peak integral).

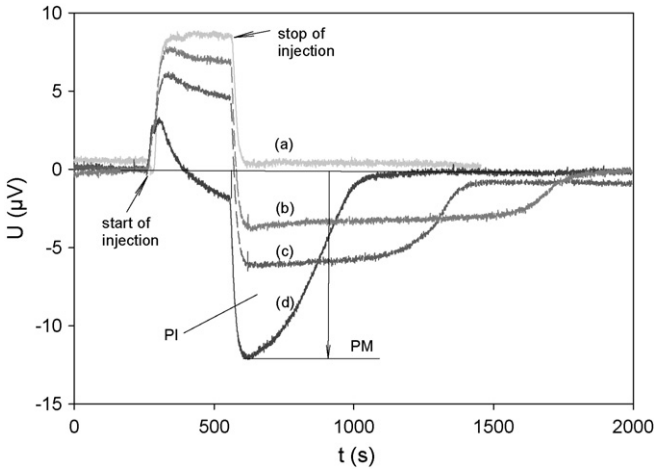

Fig. 5. Calorimetric signals obtained from a biofilm of changing activity (b–d). Signal (a) is from a sterile chamber. PM and PI are the peak magnitudes related to the base line and the voltage integral of the exothermal part of the signal, respectively [12].

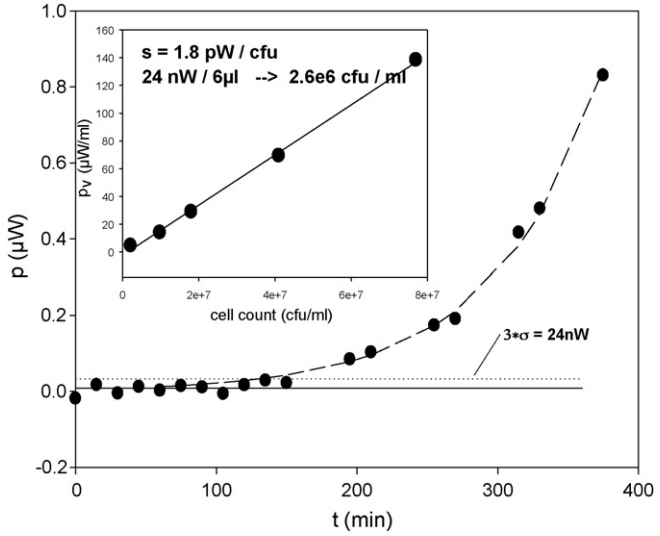

Fig. 6. Calorimetrically determined growth curve of the strain *Staphylococcus aureus* at low cell concentration. The plotted heat flow data were obtained from the signal shifts SS according to Fig. 4. The insert depicts the correlation of the metabolic heat production and the cell count (cfu: colony forming units).

ment of a bacterial suspension diluted to about $10^5\,ml^{-1}$. After injection of the suspension the signal shift SS indicates a steady-state exothermal heat production. In order to restore the base line the bacteria suspension has to be removed by a second injection step. The signal shift which is the measure of the metabolic heat production is obtained by interpolation between the base line levels before and after the two injections, respectively. The signal depicted in Fig. 3B was obtained from measurements of the metabolic activity of a biofilm. The signal independently returns to the base line due to oxygen depletion, which is the consequence of the aerobic nature of the metabolism of the investigated organisms. The signals obtained from the embryo measurements are similar.

The base line noise derived from a period of 10 min is about 60 nV, i.e. close to the physical limits. The signal shift measured during injection is an effect of internal temperature gradients caused by the non-uniform heat power dissipation inside the carrier platform of the inner thermostat. Therefore, this injection effect increases with the controller heat power P2 ($0.35\,\mu V\,mW^{-1}$). Furthermore, there is a remaining impact of the ambient temperature on the base line and the injection effect because the chip module is not perfectly shielded by the inner thermostat (weak thermal coupling of the removable lids of the thermostat). We found values of $-0.1\,\mu V\,K^{-1}$ and $-0.5\,\mu V\,K^{-1}$ for the temperature dependence of the base line and the injection effect, respectively. In some applications, e.g. in the study of highly active biofilms, signals must be analyzed immediately during fluid injection. Therefore, some need for a further reduction and stabilization of the injection effect exists, which could be done for instance by a more sophisticated spreading of the thermostat controller elements. The long-term stability of the calorimeter was tested by periodical injection of an inert fluid (nutrient solution) for 12 h. A variation was found for the signal shift SS of 0.1 µV (standard deviation) corresponding to 20 nW. Deviations are mainly caused by ambient temperature fluctuations as was indicated by the controller heat power development of the outer thermostat. The use of a chamber with an inert insertion at TP4 position allows the common mode rejection of external temperature perturbations and leads to an reduction of the data scatter down to 50 nV (10 nW).

3.3. Measurement examples

Three measurement examples should demonstrate the potential of the device presented. The signals depicted in Fig. 5 correspond to a growing biofilm of *P. putida*. From plot (b–d) the endother-

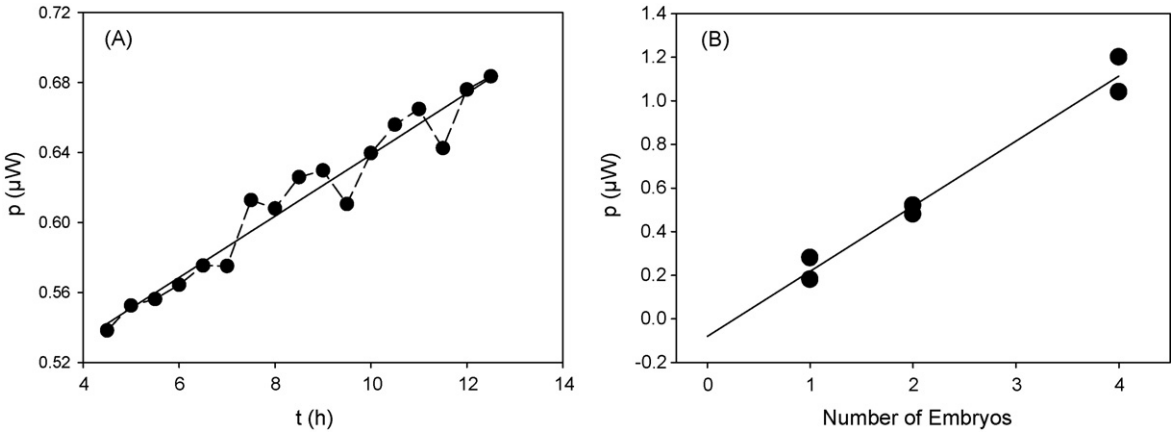

Fig. 7. Metabolic heat production of zebra fish embryos. (A) Monitoring of the growth of three embryos by measuring of the change of the metabolic rate. (B) Dependence of the metabolic heat production on the number of the embryos (24–27 h after fertilization).

mal injection effect is increasingly compensated by the exothermal heat production of the bacteria. Plot (a) was measured with a sterile chamber. The exothermal heat flow peak observed after stop of injection is a measure of the activity of the biofilm. Since the amount of oxygen available inside the chamber is limited, the decay of the signal accelerates with increasing activity of the biofilm. From the correlation of heat flow and cell count, a cell specific heat production of 0.13 pW cell^{-1} was obtained. This value is more than one order smaller than those found for planktonic growing *P. putida* [12]. It is an impressive demonstration of the reduced metabolic activity of mature biofilms.

The calorimetrically determined growth curve of suspended *Staphylococcus aureus* is shown in Fig. 6. A heat power equivalent noise level of 8 nW was observed during the measurement series. From the correlation of the heat flow and the cell count a cell specific heat production of 1.8 pW cell^{-1} results which corresponds to a cell count related limit of detection of 10^6 cells ml^{-1}.

Calorimetric measurements with single fish embryos were performed for the first time. Fig. 7A shows the change of the metabolic heat production caused by the growth of the embryos. The correlation of the heat production and the number of implemented embryos (Fig. 7B) provides a specific value of 200 nW/embryo.

4. Conclusions

With the described instrument we can demonstrate that the construction of chip calorimeters with nano-Watt resolution is possible even when the sample size is a few micro-litres and a flow-through regime is applied. To our knowledge the obtained limit of detection of 10 nW is the best value so far. This low detection limit is especially relevant for microbiological applications. The monitoring of the heat production of suspended and associated bacteria at this level of detection will allow sophisticated investigations of the physiological state of the organisms in an affordable frame. The calorimetrically based quantification of anti-biofilm agents becomes a realistic alternative to conventional microbiological methods. A calorimeter as described could be incorporated into the feedback control of a bioreactor. Since individual small multi-cellular organisms can also be investigated, micro-sized calorimetry could provide a promising platform for the screening of pharmaceutical agents.

In the future further optimizations can be expected, especially in respect to the measurement performance during the injection phase. If high-density cultures have to be investigated via an online connected chip calorimeter the sample transfer time has to be decreased below 30 s, which will be possible only in continuous flow regime. Furthermore, the adaptation of new fluidic technologies as for example *segmented flow* techniques [14] will reduce cross-talk effects between sequentially injected samples.

Acknowledgements

Financial support of the German Research Council (Deutsche Forschungsgemeinschaft, Le1128/1-1, Ma3746/2-1) and German Federation of Industrial Research Associations (AiF BMWi, AiF-Nr. 244 ZBG) is gratefully acknowledged. Dr. A. Steinhuber and Prof. A. Trampuz (University Hospital Basel, CH) are acknowledged for their collaboration in the investigations of *Staphylococcus aureus*.

References

[1] T. Maskow, H. Harms, Eng. Life Sci. 6 (2006) 266–277.
[2] J. Lerchner, T. Maskow, G. Wolf, Chem. Eng. Process. 47 (2008) 991–999.
[3] J. Lerchner, A. Wolf, G. Wolf, I. Fernandez, Thermochim. Acta 446 (2006) 168–175.
[4] E.A. Johannessen, J.M.R. Weaver, L. Bourova, P. Svoboda, P.H. Cobbold, J.M. Cooper, Anal. Chem. 74 (2002) 2190–2197.
[5] Y. Zhang, S. Tadigadapa, Biosens. Bioelectron. 19 (2004) 1733–1743.
[6] J. Higuera-Guisset, J. Rodriguez, M. Chacon, Thermochim. Acta 427 (2004) 187–191.
[7] K. Verhaegen, K. Baert, J. Simaels, W. van Driessche, Sens. Actuators A82 (2000) 186–190.
[8] F.E. Torres, P. Kuhn, D. de Bruyker, A.G. Bell, M.V. Wolkin, E. Peeters, J.R. Williamson, G.B. Anderson, G.P. Schmitz, M.I. Recht, S. Schweizer, L.G. Scott, H.J. Ho, S.A. Elrod, P.G. Schultz, R.A. Lerner, R.H. Bruce, PNAS 101 (2004) 9517–9522.
[9] J. Lerchner, A. Wolf, G. Wolf, V. Baier, E. Kessler, M. Nietzsch, M. Krügel, Thermochim. Acta 445 (2006) 144–150.
[10] V. Baier, R. Foedisch, A. Ihring, E. Kessler, J. Lerchner, G. Wolf, J.M. Koehler, M. Nietzsch, M. Kruegel, Sens. Actuators A (2005) 354–359.
[11] M.A.A. O'Neill, A.E. Beezer, C. Labetoulle, L. Nicolaides, J.C. Mitchell, J.A. Orchard, J.A. Connor, R.B. Kemp, D. Olomolaiye, Thermochim. Acta 399 (2003) 63–71.
[12] J. Lerchner, A. Wolf, F. Buchholz, F. Mertens, H. Harms, T. Neu, T. Maskow, J. Microbiol. Methods 74 (2008) 74–81.
[13] A. Funfak, J. Lerchner, J.M. Köhler, Proceedings of the Fourth Workshop Chemical and Biological Micro Laboratory Technology, Ilmenau, Germany, 2008.
[14] J.M. Köhler, U. Dillner, A. Mokansky, S. Poser, T. Schulz, Proceedings of the Second International Conference on Microreaction Technology, New Orleans, USA, 1998, S. 241.